Research on
Engineering
Structures & Materials
journal homepage: http://jresm.org

RESEARCH
GROUP

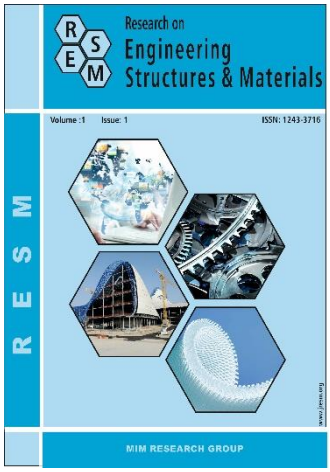

Elastic-plastic deformation of a thin rotating solid disk of exponentially varying density

Manoj Sahni, Sanjeev Sharma

Online Publication Date: 05 Sep 2016
URL: http://dx.doi.org/10.17515/resm2016.41me0401.html
DOI: http://dx.doi.org/10.17515/resm2016.41me0401

Journal Abbreviation: *Res. Eng. Struct. Mat.*

To cite this article
Sahni M, Sharma S. Elastic-plastic deformation of a thin rotating solid disk of exponentially varying density. *Res. Eng. Struct. Mat*., 2017; 3(2): 123-133

Research on
Engineering
Structures & Materials
journal homepage: http://jresm.org

RESEARCH
GROUP

Research Article

Elastic-plastic deformation of a thin rotating solid disk of exponentially varying density

Manoj Sahni*[1], Sanjeev Sharma[2]

[1] *Department of Mathematics & Computer Science, SoT, PDPU, Gandhinagar-382007, Gujarat, India*
[2] *Department of Mathematics, JIIT, A-10, Sector-62, Noida-201307, India*

Article Info

Article history:
Received 01 Apr 2016
Revised 21 Jun 2016
Accepted 05 Sep 2016

Keywords:
Elastic-plastic,
Rotating disk,
Density,
Strain hardening,
Stresses

Abstract

The plane state of stress in an elastic-plastic rotating solid disk of exponentially varying density is studied. Elastic-plastic stresses and displacement have been derived using Tresca's yield condition, its associated flow rule and linear strain hardening. Results obtained have been discussed numerically and depicted graphically for different geometric parameters. The results for uniform density are verified with those available in literature. It is observed that with the variation in density exponentially (decreases radially), high angular speed is required for a material to become fully plastic which in turns give more significant and economic design by an appropriate choice of density parameters.

1. Introduction

The use of rotating disks in machinery and structural applications has generated considerable interest in many problems in the domain of solid mechanics. There are many applications of such type of rotating disks, such as, high speed gears, turbines rotors, flywheels, disk drives. Naturally with all these applications and interest, there has been much research in this field and included in many textbooks such as [1] and [2]. The stress distribution in an elastic-plastic rotating solid disk was first studied in 1925 [3]. The usual approach for the determination of the elastic-plastic stress distribution is to apply the principle of momentum, Hooke's law, Tresca's yield condition and the condition of vanishing of radial stress at the outer surface of the disk. The first modern treatment for the elastic-plastic annular and solid disk with linear strain hardening has been introduced in 1983 [4]. It was shown in 1983 that the analysis based on Tresca's yield condition for the elastic-perfectly plastic rotating solid disk is not meaningful. Accordingly, it was shown in 1984 that a meaningful solution for linear strain hardening can be obtained. In the analysis of 1983 and 1984, the plastic region of the disk in the elastic-plastic state consists of two plastic regimes with different forms of the yield condition, the inner being a corner regime and the outer a side regime of Tresca's hexagon. However, it is well known that disks with variable thickness and variable density, and other cases, are frequently found in mechanical engineering. Over the last thirty years more and more effort has been devoted to the analysis of elastic-plastic strain-hardening rotating disks with constant or variable density and thickness. Following the approach introduced in 1984 by Gamer, the work extended in 1993 and 1995 [5-6], to solid and annular disks with variable thickness and variable density subjected to different conditions. It is shown in 1999 [7] that Tresca criterion supplies a more conservative solution and the use of elliptical parameters with von-Mises criterion is convenient for a Runge-Kutta numerical solution. Further a unified numerical method [8] is employed for the elastic-plastic nonlinearly strain hardening rotating solid disks of constant thickness and for annular disks of variable thickness and

*Corresponding author: manoj_sahani117@rediffmail.com
DOI: http://dx.doi.org/10.17515/resm2016.41me0401

variable density. In 2002 [9] a problem on elastic-plastic rotating solid disk taking the variation of thickness in an exponential form is solved. A new approach was developed using asymptotic phenomena by Seth in 1960's and is used for problems related to disc, cylinders and shells, etc. The theory was well applied by different researchers [10-15].

The motivation behind carrying out this work is to increase or decrease the hardness and strength of the disk from inner to outer radii with the change in density parameter. Most of the work done on variation in density is related to linear or parabolic profile. The work reported in this paper consider disk with exponential variable density and constant thickness. The materials usually have different densities, and density may be relevant to buoyancy and purity.

In this paper, the behavior of linear strain hardening isotropic material of rotating solid disk with variable density in an exponential form is studied under Tresca's yield condition and its associated flow rule.

2. Basic Equations and Solution of Problem

We consider a state of plane stress and assume infinitesimal deformation. Cylindrical polar coordinates *r,* θ and *z* are employed. The thickness of the disk is assumed to be constant and its density profile vary radially in an exponential form given by

$$\rho = \rho_0 e^{-n\left(\frac{r}{b}\right)^k} \tag{1}$$

where ρ_0 is the density at the axis, *k* and *n* are geometric parameters and *b* is the radius of the disk. The elastic-plastic solid disk is divided into three regions, where the plastic core consists of two parts with different forms of the yield condition. Here r_1 and r_2 are the interface radii separating the two plastic regions and the outer elastic region, respectively.

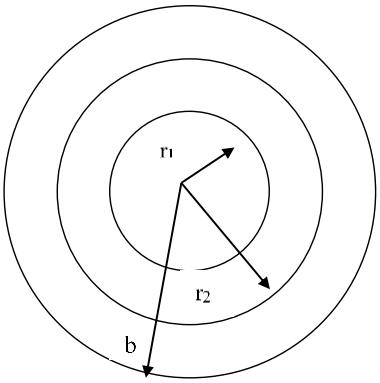

Fig. 1. Solid disk showing the interface radii r_1 and r_2

2.1. Inner Plastic Region $\left(0 \le r \le r_1\right)$

In this inner plastic region the stress state lies in a corner regime of Tresca's hexagon and hence the radial stress is equal to the circumferential stress. According to Tresca's yield condition, these stresses are equal to the yield stress

$$\sigma_r = \sigma_\theta = \sigma_y \tag{2}$$

The governing differential equation of motion is

$$\frac{d}{dr}\left(r\sigma_r\right) - \sigma_\theta + \rho(r)\omega^2 r^2 = 0 \tag{3}$$

where $\rho(r)$ is the density of the material occupying the annular region and ω is constant angular velocity of rotation.

Using equations (1) and (2) in (3), and integrated once to yield

$$\sigma_r = \sigma_\theta = C_1 - \rho_0 \omega^2 I_1(r) \tag{4}$$

where

$$I_1(r) = \int_0^r \xi\, e^{-n\left(\frac{\xi}{b}\right)^k} d\xi \tag{5}$$

For a linearly strain hardening material behavior the yield stress is

$$\sigma_y = \sigma_0\left(1 + \eta\varepsilon_{EQ}\right) \tag{6}$$

where σ_0 is the initial tensile yield stress, η is the work-hardening parameter and ε_{EQ} is the equivalent plastic strain. Consideration of the equivalence of increment of plastic work,

$$\sigma_\theta d\varepsilon_\theta^p + \sigma_r d\varepsilon_r^p = \sigma_y d\varepsilon_{EQ} \tag{7}$$

together with the yield condition, leads to

$$\varepsilon_{EQ} = \varepsilon_\theta^p + \varepsilon_r^p = \frac{1}{\eta}\left(\frac{\sigma_y}{\sigma_0} - 1\right) \tag{8}$$

For axisymmetric problems with small strains, the geometric relations between strain and radial displacement are $\varepsilon_r = \frac{du}{dr}$ and $\varepsilon_\theta = \frac{u}{r}$ which holds in the entire solid disk irrespective of material behavior. The total strain can be decomposed into their elastic and plastic components

$\varepsilon_r = \varepsilon_r^e + \varepsilon_r^p$ and $\varepsilon_\theta = \varepsilon_\theta^e + \varepsilon_\theta^p$ in which the superscript '*e*' and '*p*' denotes elastic and plastic components, respectively.

Decomposing the total strain into their elastic and plastic parts and using strain displacement relations one obtains,

$$\frac{1}{r}\frac{d}{dr}(ru)=\left[\frac{1}{\eta\sigma_0}+\frac{2(1-\nu)}{E}\right]\sigma_y-\frac{1}{\eta} \tag{9}$$

and therefore the displacement

$$u(r)=\left[\frac{1}{\eta\sigma_0}+\frac{2(1-\nu)}{E}\right]\left[\frac{1}{r}\int_0^r\sigma_y(\xi)\xi\,d\xi\right]-\frac{r}{2\eta}+\frac{C_2}{r} \tag{10}$$

It should be noted that

$$\lim_{r\to0}\left[\frac{1}{r}\int_0^r\sigma_y(\xi)\xi\,d\xi\right]=\lim_{r\to0}\frac{\frac{d}{dr}\left[\int_0^r\sigma_y(\xi)\xi\,d\xi\right]}{\frac{d}{dr}[r]}=\lim_{r\to0}\left[r.\sigma_y(r)\right]=0 \tag{11}$$

where σ_y is finite at the axis. The displacement at r = 0 must vanish and hence the integration constant $C_2=0$. Substituting $\sigma_y(r)=\sigma_r(r)$ into equation (10), the displacement becomes

$$u(r)=\left[\frac{1}{\eta\sigma_0}+\frac{2(1-\nu)}{E}\right]\left[\frac{rC_1}{2}-\frac{\rho_0\,\omega^2}{r}I_2(r)\right]-\frac{r}{2\eta} \tag{12}$$

where

$$I_2(r)=\int_0^r\left(\int_0^a e^{-n\left(\frac{\xi}{b}\right)^k}\xi\,d\xi\right).a\,da \tag{13}$$

The plastic strain components are obtained by subtracting their elastic parts from their total strains as

$$\varepsilon_\theta^p=\frac{u}{r}-\left(\frac{1-\nu}{E}\right)\sigma_r \tag{14}$$

$$\varepsilon_r^p=\frac{du}{dr}-\left(\frac{1-\nu}{E}\right)\sigma_r=\left[\frac{1}{\eta\sigma_0}+\frac{1-\nu}{E}\right]\sigma_r-\frac{u}{r}-\frac{1}{\eta} \tag{15}$$

$$\varepsilon_z^p=-\frac{1}{\eta}\left(\frac{\sigma_y}{\sigma_0}-1\right) \tag{16}$$

2.2. Outer plastic region $(r_1\le r\le r_2)$

In this region, stresses lie in a side regime of Tresca's hexagon with $\sigma_\theta>\sigma_r>0$. According to Tresca criterion, the largest stress is equal to the yield stress (σ_y)

$$\sigma_y = \sigma_\theta \tag{17}$$

Considering the increment of plastic work gives $\varepsilon_{EQ} = \varepsilon_\theta^p$; and according to the flow rule associated with the yield condition, equation (17), $\varepsilon_\theta^p = -\varepsilon_z^p$ and $\varepsilon_r^p = 0$. Since the radial strain is purely elastic and $\varepsilon_\theta^p = \frac{1}{\eta}\left(\frac{\sigma_\theta}{\sigma_0} - 1\right)$, the strain displacement relations lead to

$$\frac{u}{r} = \frac{1}{E}\left(\frac{1}{W^2}\sigma_\theta - \nu\sigma_r - \frac{\sigma_0}{H}\right) \tag{18a}$$

$$\frac{du}{dr} = \frac{1}{E}\left(\sigma_r - \nu\sigma_\theta\right) \tag{18b}$$

where $H = \frac{\eta\sigma_0}{E}$ is the normalized hardening parameter and $W^2 = \frac{H}{1+H}$. Solutions of equations (18a) and (18b) simultaneously for σ_r and σ_θ yields

$$\sigma_r = \frac{W^2\nu\sigma_0}{H\left(1-W^2\nu^2\right)} + \frac{EW^2}{\left(1-W^2\nu^2\right)}\left(\frac{\nu u(r)}{r} + \frac{u'(r)}{W^2}\right) \tag{19}$$

$$\sigma_\theta = \frac{W^2\sigma_0}{H\left(1-W^2\nu^2\right)} + \frac{EW^2}{\left(1-W^2\nu^2\right)}\left(\frac{u(r)}{r} + \nu u'(r)\right) \tag{20}$$

in which a prime denotes differentiation with respect to the radial coordinate '*r*'. Substituting equation (19) and (20) in the equation of motion, i.e. equation (3), the following differential equation for $u(r)$ is obtained:

$$r^2\frac{d^2u}{dr^2} + r\frac{du}{dr} - W^2u(r) = \frac{1}{E}\left[\frac{W^2\sigma_0(1-\nu)}{H}r - \rho_0\omega^2\left(1-W^2\nu^2\right)r^3e^{-n\left(\frac{r}{b}\right)^k}\right] \tag{21}$$

The above equation is Cauchy Euler's ordinary differential equation

Let $r = e^z$, $z = Log(r)$ we get,

$$u(r) = C_3r^W + C_4r^{-W} + \frac{W^2}{1-W^2}\frac{\sigma_0}{HE}(1-\nu)r - \frac{\rho_0\omega^2\left(1-W^2\nu^2\right)}{2EW}\left[r^W\int_{r1}^{r}\xi^{2-W}e^{-n\left(\frac{\xi}{b}\right)^k}d\xi - r^{-W}\int_{r1}^{r}\xi^{2+W}e^{-n\left(\frac{\xi}{b}\right)^k}d\xi\right] \tag{22}$$

Substituting (22) in equations (19) and (20), we get the radial and circumferential stresses. Finally, the plastic strain components for this region are given by

$$\varepsilon_r^p = 0\ , \qquad \varepsilon_\theta^p = \frac{1}{\eta}\left(\frac{\sigma_\theta}{\sigma_0} - 1\right) \quad \text{and} \quad \varepsilon_z^p = -\frac{1}{\eta}\left(\frac{\sigma_\theta}{\sigma_0} - 1\right) \tag{23}$$

2.3 Elastic Region $(r_2 \le r \le b)$

For elastic behavior, the stress-displacement relations becomes

$$\sigma_r = \frac{E}{(1-\nu^2)}\left(\frac{\nu\, u(r)}{r} + u'(r)\right) \tag{24a}$$

$$\sigma_\theta = \frac{E}{(1-\nu^2)}\left(\frac{u(r)}{r} + \nu\, u'(r)\right) \tag{24b}$$

Substitution of these in the equation of motion leads to

$$r^2\frac{d^2u(r)}{dr^2} + r\frac{du(r)}{dr} - u(r) = -\frac{\rho_0\omega^2(1-\nu^2)r^3 e^{-n\left(\frac{r}{b}\right)^k}}{E} \qquad \text{b} \tag{25}$$

The above equation is a non-homogeneous Cauchy Euler's ordinary differential equation, whose solution is given as

$$u(r) = C_5\, r + C_6\, r^{-1} - \frac{\rho_0\omega^2(1-\nu^2)}{2E}\left[r\int_{r2}^{r} \xi\, e^{-n\left(\frac{\xi}{b}\right)^k} d\xi - r^{-1}\int_{r2}^{r} \xi^3 e^{-n\left(\frac{\xi}{b}\right)^k} d\xi \right] \tag{26}$$

The radial and circumferential stresses can be obtained from equations (24a) and (24b), respectively.

3. Determination of Integration Constants

The expressions for stresses and displacement for different regions of deformation contain the unknown integration constants C_1, C_3, C_4, C_5, C_6 and the interface radii r_1 and r_2. For the determination of these seven unknowns there are seven nonredundant conditions available: σ_θ, σ_r and u are individually continuous at r_1 and r_2, and σ_r vanishes at the outer boundary of the disk, i.e. at r = b. Using the superscripts 'ip', 'op' and 'el' for inner plastic region $(0 \le r \le r_1)$, outer plastic region $(r_1 \le r \le r_2)$ and elastic region $(r_2 \le r \le b)$ respectively, these conditions are written explicitly as

$$u^{ip}(r_1) = u^{op}(r_1), \quad \sigma_r^{ip}(r_1) = \sigma_r^{op}(r_1), \quad \sigma_\theta^{ip}(r_1) = \sigma_\theta^{op}(r_1), \quad u^{op}(r_2) = u^{el}(r_2)$$
$$\sigma_r^{op}(r_2) = \sigma_r^{el}(r_2), \quad \sigma_\theta^{op}(r_2) = \sigma_\theta^{el}(r_2), \quad \sigma_r^{el}(b) = 0 \tag{27}$$

4. Numerical Illustration and Discussion

The results have been calculated by using MATHEMATICA. Curves are drawn for radial and circumferential stresses, displacements, plastic strains (radial and circumferential) with respect to radii ratio. Calculations are performed for two cases:

1) Disk with uniform density, 2) Disk with variable (exponentially) density. For the uniform density disk equations are same as that of Gamer of 1983 (Gamer 1983).

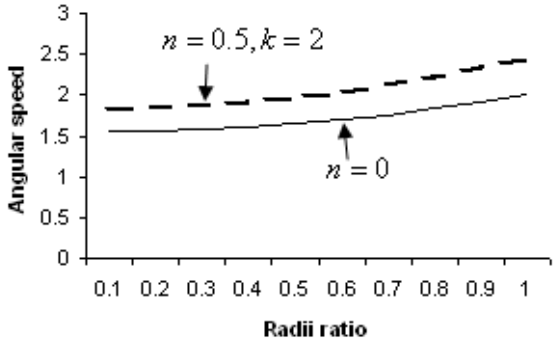

Fig. 2. Angular speed against radii ratio

From Fig. 2 we can see that for the disk with uniform density i.e. n = 0 with hardening parameter as H = 1/3, angular speed required for initial yielding is Ω_1 = 1.48735 and angular speed required for fully plastic case is Ω_2 = 2.01571. The results obtained by Gamer are Ω_1 = 1.54919 and Ω_2 = 2.08043 for n = 0, H = 0.5 and Ω_2 = 1.73195 for H = 10^{-6}. The variation compared to our results is because of the reason that angular speed for hardening material must be greater than that of non-hardening material i.e. 2.08043 (H = 1/2) > 2.01571 (H = 1/3) > 1.7195 (H = 10^{-6}). For an exponentially variable density disk (n = 0.5, k = 2), the angular speed required for initial yielding is Ω_1 =1.8153 and angular speed required for fully plastic state is Ω_2 = 2.44011 which is very high as compared to the disk with uniform density.

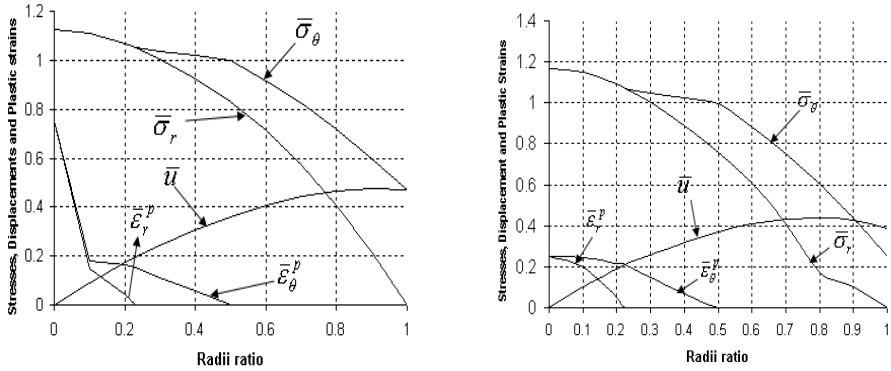

(a) (b)

Fig. 3. Normalized stresses and displacement for partially plastic case with (a) uniform density disk (n = 0, H = 0.5) and (b) variable density disk (H = 1/3, n = 0.5, k = 2).

For the partially plastic case with uniform density (H = 1/3, n = 0 and $\bar{r}_2$ = 0.5), the integration constants in non-dimensional form are $\bar{C}_1 = \frac{C_1}{\sigma_0} = 1.12341$, $\bar{C}_3 = \frac{C_3}{b^{1-W}} = 0.0619449$, $\bar{C}_4 = \frac{C_4}{b^{1+W}} = 0.00662599$, $\bar{C}_5 = C_5 = 0.610717$, $\bar{C}_6 = \frac{C_6}{b^2} = 0.0279746$ with interface radii $\bar{r}_1$ = 0.22921 and corresponding angular velocity is Ω = 1.65464 while for the disk with variable density (H = 1/3, n = 0.5, $\bar{r}_2$ = 0.5 , k = 2), the integration constants in non -dimensional form are $\bar{C}_1 = 1.16683$, $\bar{C}_3 = 0.0828$, $\bar{C}_4 = 0.00870242$, $\bar{C}_5 = 0.593503$, $\bar{C}_6 = 0.0365816$ with interface radii $\bar{r}_1$ = 0.225227 and corresponding angular velocity is Ω = 1.96853. Stresses, displacements and plastic strains are drawn in Fig. 3(a) with uniform density disk and Fig. 3(b) with variable density for the partially plastic case. It can be seen from Fig. 3 that radial and circumferential stresses are maximum at the internal surface and have been observed that up to the inner plastic region, stresses are same and thereafter radial stress decreases rapidly than that of circumferential stress. It has also been observed that a plastic strains vanishes at the interface radii.

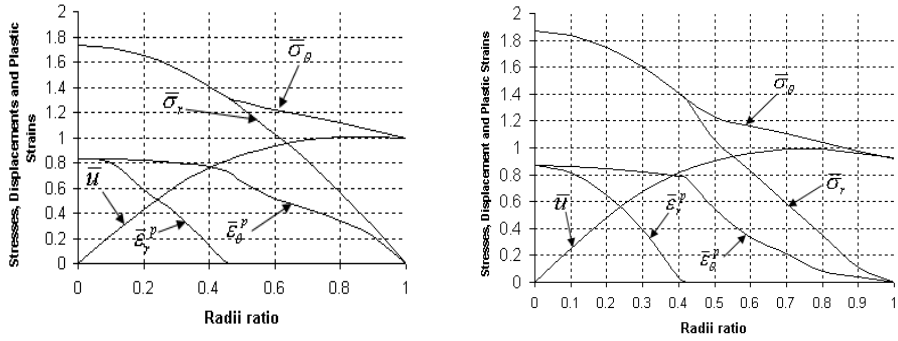

(a) (b)

Fig. 4. Normalized stresses and displacement for fully plastic case with (a) uniform density disk (n = 0, H = 0.5) and (b) variable density disk (H = 1/3, n = 0.5, k = 2).

The results for the fully plastic case are obtained using the non-redundant continuity and boundary conditions $u^{ip}(r_1) = u^{op}(r_1)$, $\sigma_r^{ip}(r_1) = \sigma_r^{op}(r_1)$, $\sigma_\theta^{ip}(r_1) = \sigma_\theta^{op}(r_1)$ and $\sigma_r^{op}(b) = 0$, where as before, the superscripts '*ip*' and '*op*' stands for inner plastic and outer plastic regions, respectively. For the fully plastic case with uniform density (H = 1/3, n = 0, $\bar{r}_2$ =1.0), the integration constants in non-dimensional form are $\bar{C}_1 = 1.73527$, $\bar{C}_3 = 0.521921$ and $\bar{C}_4 = 0.111655$ with interface radii $\bar{r}_1$ = 0.458425 and corresponding angular velocity is Ω_2 = 2.01571 while for the disk with variable density (H = 1/3, n = 0.5, $\bar{r}_2$ = 1.0, k = 2), the integration constants in non-dimensional form are $\bar{C}_1 = 1.86626$, $\bar{C}_3 = 0.584531$, $\bar{C}_4 = 0.11508$ with interface radii $\bar{r}_1$ = 0.421878 and corresponding angular velocity is Ω_2 = 2.44011. Stresses, displacements and strains are depicted in Fig. 4 for the fully plastic case.

Finally, the case beyond the fully plastic limit is studied using $H = 1/3,\ \nu = 1/2,\ k = 2,\ n = 0.5$. At the angular speed Ω_2, disk becomes fully plastic as the elastic-plastic interface radii reaches the outer boundary. However this is not the collapse speed and the disk can maintain angular velocities greater than Ω_2. The stresses and deformations occurring for two angular velocities greater than the fully plastic limit, $\Omega_2 = 2.5$ and $\Omega_2 = 3$, are given in Fig. 5.

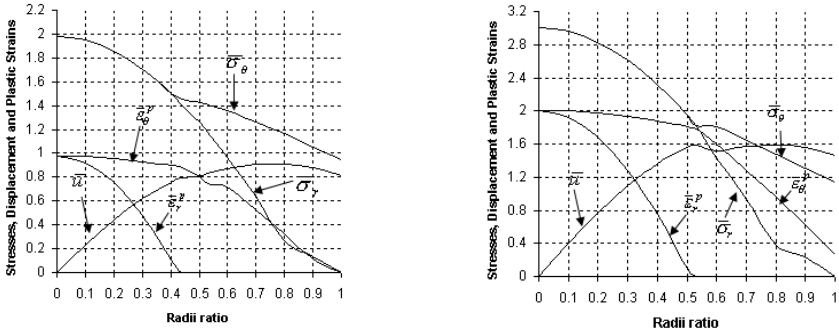

(a) (b)

Fig. 5 Normalized stresses and displacement beyond fully plastic state, $\Omega > \Omega_2$ for H = 1/3, n = 0.5, k = 2 for (a) $\Omega = 2.5$ and (b) $\Omega = 3$.

With the increase in angular speed beyond the fully plastic limit, all the parameters show a significant change. As can be seen from the figure the circumferential plastic strain becomes zero at the outer boundary for $\Omega = 2.5$ but show a significant value for $\Omega = 3$. Both the stresses increase with the increase in angular velocity. Initially the plastic strains increase and thereafter decrease. From Fig. 5, it has been observed that the magnitudes of the plastic strains are sufficiently small which justify the assumption of small deformation theory.

5. Conclusion

The results for non-hardening material is compared with those of hardening material. An analytic solution is obtained for elastic-plastic deformation of linear hardening solid disk of exponentially variable density. The results for uniform density are verified with those available in literature. It is observed that with the variation in density exponentially (decreases radially), high angular speed is required for a material to become fully plastic which in turn give more significant and economic design by an appropriate choice of density parameters.

Acknowledgement

The author wishes to acknowledge there sincere thanks to Prof. S.K. Gupta for his encouragement during the preparation of this paper.

Nomenclature:

r, θ, z	: radial, circumferential and axial directions, respectively
u	: radial displacement
b	: outer radii of the disk
r_1, r_2	: interface radii
ε_{EQ}	: equivalent plastic strain
$d\varepsilon$	: strain increment
η	: work-hardening parameter
E, ν	: Young's modulus and Poisson's ratio, respectively
n, k	: geometric parameters $\rho = \rho_0 e^{-n\left(\frac{r}{b}\right)^k}$
ω	: constant angular velocity of rotation
e, p	: superscript denoting elastic and plastic component
$\varepsilon_r, \varepsilon_\theta$	: radial and tangential strains, respectively
$\varepsilon_r^e, \varepsilon_\theta^e$	: elastic part of the strain vector
$\varepsilon_r^p, \varepsilon_\theta^p, \varepsilon_z^p$	: plastic part of the strain vector
ρ, ρ_0	: local density and density at the axis, respectively
σ_y, σ_0	: initial and subsequent yield stress, respectively
σ_r, σ_θ	: radial and circumferential stresses, respectively
C_1, C_3, C_4, C_5, C_6	: constants of integration
ip, op, el	: superscripts denoting inner plastic, outer plastic and elastic region

Dimensionless quantities:

Angular velocity: $\Omega = \sqrt{\frac{\rho_0 \omega^2 b^2}{\sigma_0}}$, Stresses: $\bar{\sigma}_{ij} = \frac{\sigma_{ij}}{\sigma_0}$, Displacement: $\bar{u} = \frac{Eu}{b\sigma_0}$

Normalized hardening parameter: $H = \frac{\eta \sigma_0}{E}$, $W^2 = \frac{H}{H+1}$

Radial co-ordinate: $\bar{r} = \frac{r}{b}$, $\bar{r}_1 = \frac{r_1}{b}$, $\bar{r}_2 = \frac{r_2}{b}$

References

[1] Fenster SK, Ugural SC. Advanced Strength and Applied Elasticity, Second Edition, Elsevier, NewYork, USA, 1987.

[2] Goodier JN, Timoshenko SP. Theory of Elasticity, Third Edition, McGraw Hill, NewYork, 1970.

[3] Laszlo F. Geschleuderte udrehungskorper im Gebiet bleibender Deformation, ZAMM, 1925; 5: 281-293. http://dx.doi.org/10.1002/zamm.19250050402

[4] Gamer U. Tresca's yield condition and the rotating solid disk, J. Appl. Mech., 1983; 50: 676 - 678. http://dx.doi.org/10.1115/1.3167110

[5] Guven U. On the stresses in an elastic–plastic annular disk of variable thickness under external pressure, Int. J. Solid Structures, 1993; 30: 651–658. http://dx.doi.org/10.1016/0020-7683(93)90027-5

[6] Guven U. On the applicability of Tresca's yield condition to the linear hardening rotating solid disk of variable thickness, ZAMM, 1995; 75: 397–398. http://dx.doi.org/10.1002/zamm.19950750510
[7] Rees DWA. Elastic-plastic stresses in rotating disks by von Mises and Tresca, ZAMM, 1999; 79: 281–288. http://dx.doi.org/10.1002/(SICI)1521-4001(199904)79:4<281::AID-ZAMM281>3.0.CO;2-V
[8] You LH, Tang YY, Zhang JJ, Zheng CY. Numerical analysis of elastic - plastic rotating disks with arbitrary variable thickness and density, Int. J. Solid Structures, 2000; 37: 7809–7820. http://dx.doi.org/10.1016/S0020-7683(99)00308-X
[9] Eraslan AN, Orcan Y. Elastic-plastic deformation of a rotating solid disk of exponentially varying thickness, Mechanics of Materials, 2002; 34: 423–432. http://dx.doi.org/10.1016/S0167-6636(02)00117-5
[10] Sharma S, Sahni M, Kumar R. Elastic-plastic transition of transversely isotropic thick-walled rotating cylinder under internal pressure, Defence Science Journal, 2009; 59: 260-264. http://dx.doi.org/10.14429/dsj.59.1519
[11] Sharma S, Sahni M. Thermo elastic-plastic transition of a homogeneous thick-walled circular cylinder under external pressure, Structural Integrity and Life, 2013; 13: 3-8.
[12] Sharma S, Sahni M. Creep analysis of thin rotating disc having variable thickness and variable density with edge loading, Annals of Faculty Engineering Hunedoara – International Journal of Engineering, 2013; 11: 289-296.
[13] Sahni M, Sahni R. Functionally graded rotating disc with internal pressure, Engineering and Automation Problems, 2014; 3: 125-130.
[14] Sharma R, Aggarwal AK, Sharma S, Sahni, M. Thermo creep transition in
[15] Sahni M, Sahni R. Rotating functionally graded disc with variable thickness profile and external pressure, Elsevier Procedia Computer Science, 2015; 57: 1249–1254. http://dx.doi.org/10.1016/j.procs.2015.07.426